

SPECIAL REPORT 90-23

DTIC COPY



①

AD-A225 955

Evaluation of PVDF Piezopolymer for Use as a Shock Gauge

Plyush K. Dutta and John Kalafut

June 1990

DTIC
ELECTE
AUG 29 1990
S B D

DISTRIBUTION STATEMENT A

Approved for public release;
Distribution Unlimited

010 010 010 010 010

For conversion of SI metric units to U.S./British customary units of measurement consult ASTM Standard E380, Metric Practice Guide, published by the American Society for Testing and Materials, 1916 Race St., Philadelphia, Pa. 19103.

Special Report 90-23



**U.S. Army Corps
of Engineers**
Cold Regions Research &
Engineering Laboratory

Evaluation of PVDF Piezopolymer for Use as a Shock Gauge

Piyush K. Dutta and John Kalafut

June 1990

PREFACE

This report was prepared by Dr. Piyush K. Dutta, Materials Research Engineer of the Applied Research Branch, Experimental Engineering Division, and John Kalafut, Electrical Engineer of the Engineering and Measurement Services Branch, Technical Services Division, U.S. Army Cold Regions Research and Engineering Laboratory. Funding was provided under the In-house Laboratory Independent Research (ILIR) Program in FY 1988.

The authors thank George Blaisdell and Donald Garfield, both of CRREL, for technically reviewing this report.

The contents of this report are not to be used for advertising or promotional purposes. Citation of brand names does not constitute an official endorsement or approval of the use of such commercial products.



Accession For	
NTIS GRA&I	<input checked="" type="checkbox"/>
DTIC TAB	<input type="checkbox"/>
Unannounced	<input type="checkbox"/>
Justification _____	
By _____	
Distribution/ _____	
Availability Codes	
Dist	Avail and/or Special
A-1	

Evaluation of PVDF Piezopolymer for Use as a Shock Gauge

PIYUSH K. DUTTA AND JOHN KALAFUT

INTRODUCTION

About a century ago, piezoelectric solids such as quartz and ceramics were discovered. They have been since used as phonograph pickups, transducers and spark igniters for gas stoves, among other things. However, they aren't universally useful. Because of their brittleness, it is difficult to make them into complex shapes, and, because of their high stiffness, they vibrate for a long time, which is undesirable in applications where rapid damping is required.

In the late 1960s the piezoelectric property of polyvinylidene fluoride (PVDF) was discovered and its potential use in sensors became apparent. Now, a commercial PVDF film (Kynar*) is available in thicknesses ranging from 28 to 110 μm . The material has several attractive properties—including light weight, flexibility, high response time and a wide frequency range—that make it superior to ceramic or other crystalline piezoelectric materials. It is so pliable that it can be shaped into just about any configuration without its piezoelectric capability being degraded. High humidity has no effect on its characteristics. PVDF film is better than quartz or ceramic as a transformer of mechanical energy to piezoelectricity or vice versa. Table 1 lists the mechanical and electrical properties of the Kynar PVDF piezofilm. Table 2 compares several key properties of this film with those of other well known piezoelectric materials.

One of the major advantages of Kynar piezofilm is its low acoustic impedance (about $1.9 \times 10^6 \text{ kg/m}^2 \text{ s}$), which matches very well with the acoustic impedance of most soils (4.6×10^6 to $1.8 \times 10^6 \text{ kg/m}^2 \text{ s}$), and thus makes it an excellent candidate for a soil shock gauge. This report will discuss the use of this material in the development of shock sensors, which will be used for measuring shock waves in frozen soil.

BACKGROUND

The phenomenon of a material's dimensions changing when it is subjected to an electric field is known as piezoelectricity (from the Greek piezo for pressure) and has been defined by Cady (1946) as polarization of

electric charge produced by mechanical strain, the polarization being proportional to the amount of strain. The reverse is also true—an applied charge will induce a mechanical strain in the material. A similar effect known as pyroelectricity is also induced in some materials—when heat is applied or removed, the induced electricity is again proportional to the level of thermal change.

By far, PVDF, whose molecular repeat formula is $(\text{CH}_2-\text{CF}_2)_n$, exhibits the strongest piezoelectric and pyroelectric activity of all known polymers (Loving 1983, Chatignij 1986). The discovery that a piezoelectric property could be induced in PVDF was first reported by Kawai (1969); Bergman (1971) discovered the pyroelectric effect.

Like all piezoelectric materials, PVDF consists of countless dipoles (regions of positive and negative charge) in random orientation. But, by a process called poling, the dipoles align by stretching and heating in the presence of an electric field.

In application, PVDF piezofilm is a composite structure, in which the PVDF film is sandwiched between two metallized films (Fig. 1). When a voltage of proper polarity is applied to the composite film, the film becomes thinner and elongates, whereas with a voltage of opposite polarity, the film contracts and thickens. On the other hand, if the film is mechanically elongated, say by application of pressure, voltage will be generated with appropriate polarity (Fig. 2). In a similar manner, if negative pressure (vacuum) is applied to the film, the opposite polarity voltage will develop. Thus, a reciprocating force (or pressure) will result in an alternating voltage output.

It should, however, be noted that the electric charge that is developed across the electrodes is proportional to the change in mechanical stress, and that this charge dissipates through the film material with time. Thus, measurement must be made within a short time after the charges are generated. There is another difficulty; the electronic circuitry at the measuring interface also provides a path for such dissipation, so it is essential to develop and use suitable electronics for precise measurements.

Like all piezoelectric materials, PVDF is also anisotropic; thus, for systematically referencing its properties, it is convenient to use a three-dimensional coordinate system. Figure 3 shows this coordinate system.

*Pennwalt Inc., King of Prussia, Pennsylvania.

Table 1. Typical room-temperature properties of Kynar piezofilm (Pennwalt Corp. 1983).

Capacitance	C	417 pF/cm ² (28- μ m film)
Specific heat	C_v	2.4×10^6 J/m ³ K
Mass density	ρ	1.78×10^3 kg/m ³
Thermal conductivity	G	0.13 W/m K
Glass transition temperature	T_g	-40°C
Young's modulus	E_{11}^y	2×10^9 N/m ²
Compressive strength	S_c	$55-70 \times 10^6$ N/m ²
Tensile strength	T_{11}	$160-330 \times 10^6$ N/m ²
Velocity of sound (transverse)	T_{33}	$30-55 \times 10^6$ N/m ²
Piezoelectric voltage constants	C_v	$1.15-2.2 \times 10^3$ m/s
	g_{31}	0.216 (N/m)/(V/m ²)
	g_{32}	0.019 (N/m)/(V/m ²)
	g_{33}	-0.339 (N/m)/(V/m ²)
	g_h	-0.104 (N/m)/(V/m ²)
	g_i	-0.207 (N/m)/(V/m ²)
Maximum operating temperature		80°C
Minimum operating temperature		-40°C

If tension is applied to the 1-1 direction or the 2-2 direction, surface 3-3 is free to contract and charges will develop on these 3-3 surfaces. Also, if a pressure is applied in the 3-3 direction, the film is free to expand in the 1-1 and 2-2 directions and charges will develop on the 3-3 surface. The electrical voltage output for a given thickness t of piezofilm with stress σ is given by

$$V = g_{33} \sigma t \quad (1)$$

where V is the induced electrical voltage and g_{33} is the piezoelectric voltage constant specific to the film under consideration. Pressure here is applied in the 3-3 direc-

tion. The constant g_{33} value is expressed in volts per meter per newton per square meter (V/m)/(N/m²).

For Kynar piezofilm the value of g_{33} varies from -0.339 (unconstrained) to -0.207 (V/m)/(N/m²) (constrained) (Pennwalt Corp. 1983). (The negative sign relates to application of a compressive force.) Thus, an unconfined piezofilm, having a thickness of 28 μ m (0.001 in.), when subjected to a 10-MN/m² tensile strength will induce a voltage computed from eq 1 of 95 V. For the same circumstances, a confined film will produce 58 V. Note that the voltage output increases with applied stress and also increases with the thickness of the piezofilm.

Table 2. Comparative properties of Kynar PVDF and other piezoelectric materials.

Materials	Cut orientation	Density ρ (kg/m ³)	Elastic constant E (N/m ²)	Piezoelectric constant g_{33} ($\frac{V/m}{N/m^2}$)	Acoustic impedance ($\frac{\rho c}{m^2/s}$)
Quartz	X	2.65×10^3	77.2×10^9	50×10^{-3}	14.3×10^6
Rochelle salt	45°X	1.77×10^3	17.7×10^9	90×10^{-3}	5.6×10^6
B ₂ TiO ₅	Z	5.7×10^3	110×10^9	5.2×10^{-3}	30×10^6
Kynar	Z	1.78×10^3	2×10^9	200×10^{-3}	1.9×10^6

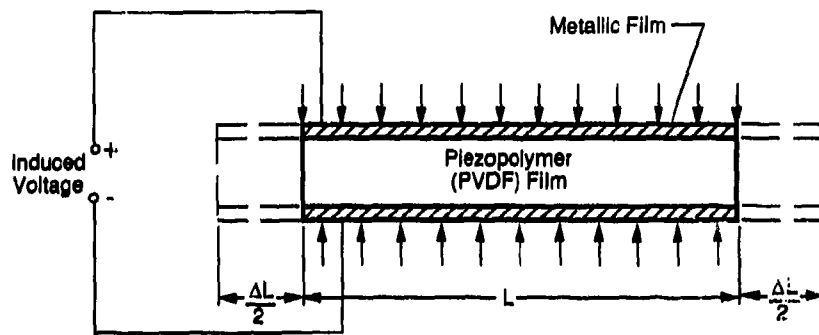


Figure 1. Principle of operation of piezopolymer film.

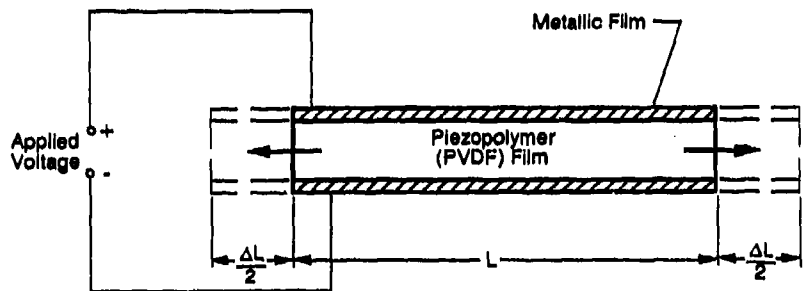


Figure 2. Induced voltage from applied pressure on piezofilm.

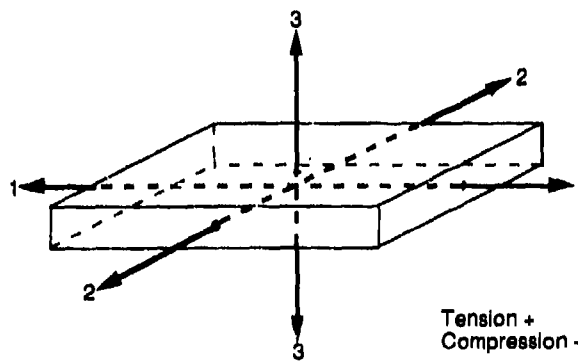


Figure 3. Coordinate system of the anisotropic PVDF material.

FABRICATION OF THE SHOCK GAUGE

We fabricated shock gauges for monitoring shock pressure attenuation in a frozen column of soil using Pennwalt model DT1-028K 40- by 15-n.m films that were 28 μm thick and supplied with silver paint metallization. As received from the manufacturer, the material is extremely delicate. Projecting out of the film are two tabs to which lead wires must be attached. Gauges with attached lead wires are available but they are comparatively more expensive. The commercial process to attach leads uses a riveted connection; the added bulk is not suitable for an inclusion gauge.

Our procedure for attaching lead wires and preparing the gauge for embedding in the frozen soil sample is simple (Fig. 4). The film is first placed flat on a surface, and one of the two tinned lead wires is brought into contact with the metal foil tab, using adhesive tape to keep the wire in position. With a fine brush, a dab of 1-mm-diameter silver conductive paint is placed on the tinned lead wires in contact with the tab. The paint is allowed to dry for about 6 hours. The paint has very little mechanical strength; therefore, a drop of clear epoxy was used to provide the mechanical strength. After an overnight cure, the lead wire gains sufficient strength for impact calibration. After the epoxy has cured, continuity between the metallized surface and the lead wire terminal is checked. The operation is repeated for both metal tabs.

Two batches of gauges were manufactured using the 28- μm -thick Kynar film. The first batch had a nominal

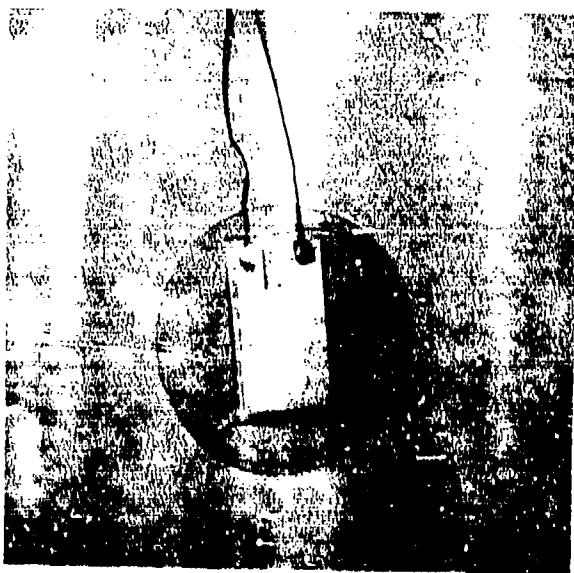


Figure 4. PVDF gauge prepared for embedding in soil sample before freezing.

Table 3. Capacitance values of shock gauges.

Batch A (30 \times 12 mm)		Batch B (30 \times 12 mm)	
Gauge no.	Capacitance (pF)	Gauge no.	Capacitance (pF)
05	1250	16	1190
06	1200	17	771
07	1180	18	809
08	1140	19	791
09	1250	20	662
10	1180	21	685
11	1180		
12	1210	23	652
13	1310	24	636
14	1260	25	637
15	1280		
		27	660
		28	690
		29	705

size of 30 by 12 mm. To protect the metallized surface and insulate it from moisture when the gauge is embedded in soil, both sides of the gauge were coated with Micromasurement PCT-2 cellophane tape. As a quality check after we coated the gauges, we measured the capacitance of each gauge using a capacitance bridge. All gauges of the second batch, except gauge 16, were manufactured using 16- by 12-mm piezofilm. Gauge 16 was made 32 by 16 mm. However, for improved moisture sealing, we laminated all these gauges in a laminator machine. Table 3 lists both batches of the gauges with their capacitance values.

INSTRUMENTATION

The responses of the gauges to a shock wave were monitored on a Nicolet 4094A digital oscilloscope. The basic output of the shock gauge is an electrical charge that needs to be converted to voltage for input to the oscilloscope. This process is accomplished by the use of a charge amplifier. Also, the piezopolymer shock gauges produced a large amount of charge, requiring the use of a charge divider.

A block diagram of the instrumentation system is shown in Figure 5. The charge divider was designed and constructed at CRREL; Figure 6 shows its design. The purpose of the charge divider is to reduce the output charge proportionately to the charge generated at the sensor. This is accomplished by using two capacitors of suitable values, one parallel and another in series with the input of the charge amplifier. From Figure 6 it can

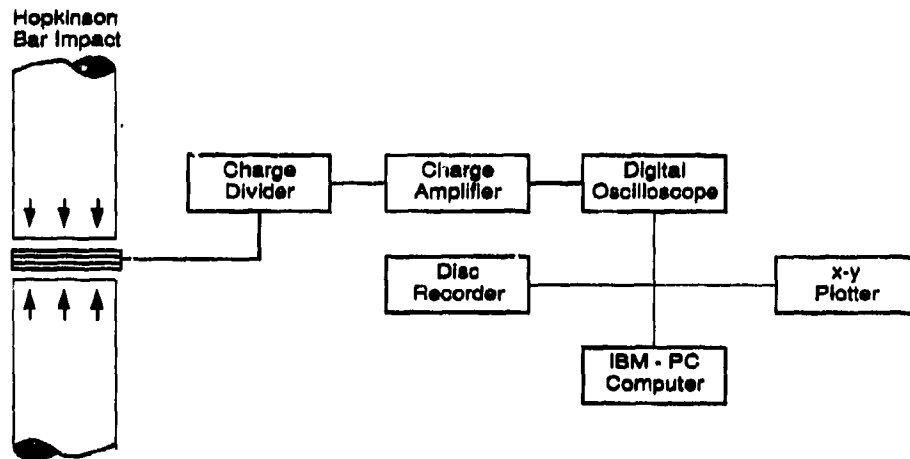


Figure 5. Instrumentation system for measuring shock pressure by the gauge.

be seen that if C_1 , C_2 and C_3 are capacitance of the gauge, parallel capacitor and series capacitor, respectively, and

Q_1 = charge generated in the shock gauge
 Q_2 = charge induced across capacitor C_2
 Q_3 = charge induced across terminals AB

then the total charge Q_T can be found from

$$Q_T = Q_1 + Q_2 + Q_3 \quad (2)$$

If V = voltage across each of these capacitors, then considering $Q_1 = VC_1$, $Q_2 = VC_2$ and $Q_3 = VC_3$, it can be seen that

$$\frac{Q_3}{Q_T} = \frac{C_3}{C_1 + C_2 + C_3} \quad (3)$$

In our application we have chosen the following values for the capacitors:

$C_1 = 1500$ pF
 $C_2 = 100,000$ pF
 $C_3 = 11,1000$ pF.

Using these values in eq 3, we calculated the charge across the charge amplifier to be 9.86% of Q_T .

In our case, the charge divider reduced the input to the charge amplifier to approximately 10% of the quantity of charge generated by the gauge.

The output from the charge divider is fed through the charge amplifier into the Nicolet Model 4094A digital oscilloscope. The data from the oscilloscope can be plotted on either an x-y plotter or permanently recorded on a floppy disk.

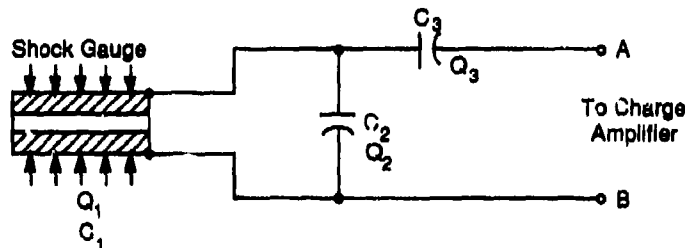


Figure 6. Circuit diagram of the charge divider.

SHOCK GAUGE CALIBRATION

Hopkinson bar apparatus

The shock gauge was calibrated in the CRREL Hopkinson bar apparatus. The apparatus has been described in detail by Dutta et al. (1987). In brief, the system consists of two long, collinear, cylindrical bars, one of which is struck by a short, solid, cylindrical striker bar. The resulting stress wave propagates through the first bar and impacts the test specimen, which is mounted between the two bars. The incident and reflected stress waves in the first bar and the transmitted stress wave in the second bar are measured by strain gauges mounted on each bar.

For calibration, the shock gauge was placed at the interface between the two bars. The test arrangement is shown in Figure 7.

Under the assumption that there is negligible attenuation of the stress wave between the interface and the foil strain gauge located on the second bar, the stress measured by the test shock gauge would be the same as the transmitted stress measured on the second bar by the foil strain gauge. The amplitude of the stress wave can be varied by changing the impact velocity of the short striker bar (which is driven by compressed air from a cylinder).

We built 30 piezopolymer gauges, including the first five prototypes for calibration tests. The following results are from the calibration tests.

Pressure calibration

We tested gauge 1 with impact force levels resulting from accelerating the striker with pressures increasing in 20-KN/m² increments from 40 to 160 KN/m². The stress wave outputs from the shock gauge and the stress waves recorded by the strain gauge mounted on bar 2 are shown in Figure 8. The numbers associated with each curve represent corresponding waveforms. Figure 9 is a plot of the calibration data given in Table 4.

One of the gauges was subjected to a repeatability test of seven successive impacts at a constant compressed air pressure of 48 KN/m². The gauge output waveform traces from these successive impacts are shown in Figure 10. Single traces from the strain gauges on bars 1 and 2 are also shown for reference. Note that successive traces from the gauge have excellent superimposition, showing reasonably good repeatability.

Because in the actual experiment the shock wave stress value in frozen soil will be much lower, about 17.5 MN/m², subsequent gauges were all calibrated at only four points, with the maximum stress level being below 17.5 MN/m². Table 5 gives the results of these calibration tests.

It is evident from Table 5 that the calibration factor varied from gauge to gauge. This is expected because of differences in the coatings, and possibly in the thicknesses of the gauges. However, the range of variation is still rather small; we can see the standard deviation is only 0.153 for the mean of 15.886 (KN/m²)/mV, and

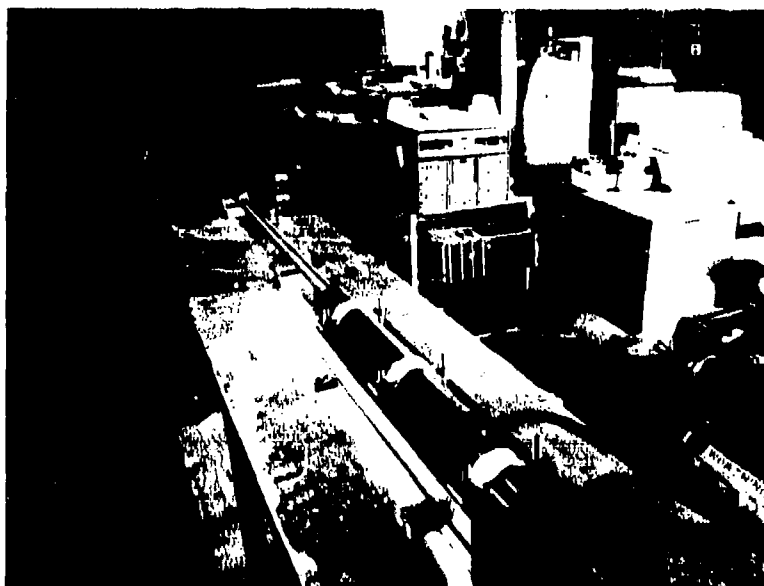


Figure 7. Shock gauge calibration test setup.

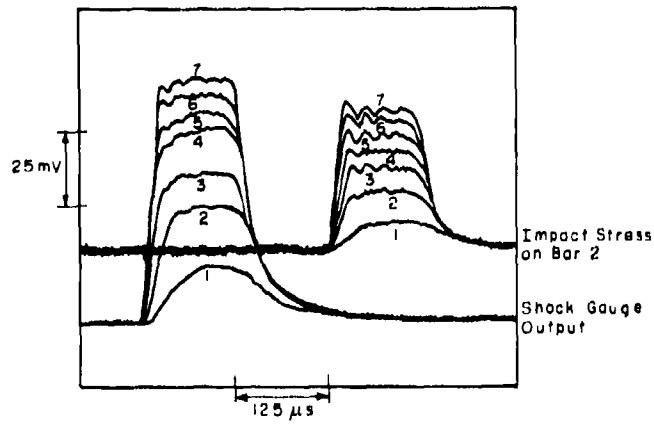


Figure 8. Comparison of impact stress and shock gauge output in Hopkinson bar test.

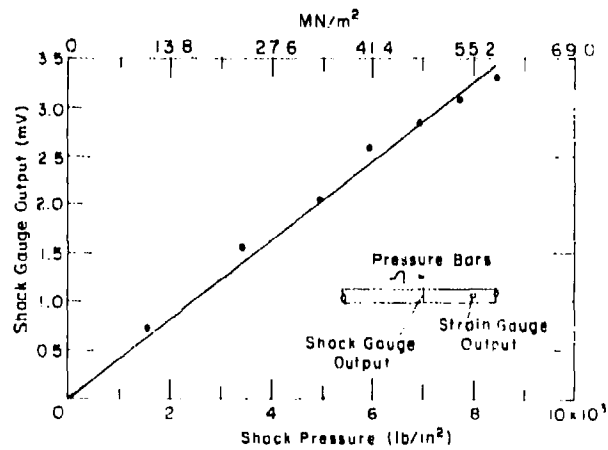


Figure 9. Typical plot of calibration data.

Table 4. Calibration data of stress vs shock gauge output.

Compressed air pressure		Incident wave*			Transmitted wave			Shock gauge peak amplitude
(lb/in. ²)	(KN/m ²)	(mV)	(lb/in. ²)	(MN/m ²)	(mV)	(lb/in. ²)	(MN/m ²)	(V)
6	41.4	9.356	1664.7	11.478	8.656	1540.1	10.619	0.731
9	62.1	20.328	3616.9	24.938	19.253	3425.6	23.619	1.56
12	82.7	29.078	5173.7	35.673	27.822	4950.2	34.132	2.042
15	103.4	35.300	6280.8	43.306	33.528	5965.5	41.132	2.858
18	124.1	40.900	7277.1	50.176	38.934	6927.3	47.764	2.841
21	144.8	45.700	8131.2	56.064	43.513	7742.1	53.381	3.085
24	165.5	49.922	8882.4	61.244	47.581	8465.8	58.372	3.301

*Hopkinson bar scale factors:

$$1 \text{ mV} = 177.925 \text{ lb/in.}^2$$

$$1 \text{ mV} = 1.226792 \text{ (N/m}^2\text{)} \times 10^6$$

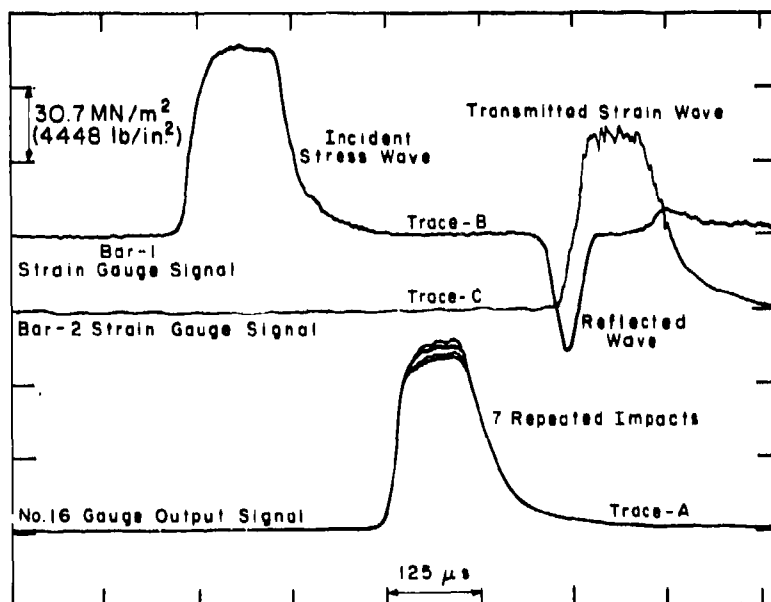


Figure 10. Repeatability test results from Hopkinson bar tests.

Table 5. Individual calibration test results of the PVDF shock gauges.

Gauge no.	Input peak stress		Gauge output (mV)	Calibration factor		Average calibration factor: F	
	(lb/in. ²)	(MN/m ²)		[(lb/in. ²)/mV]	[(KN/m ²)/mV]	[(lb/in. ²)/mV]	[(KN/m ²)/mV]
Batch A							
5	335.7	2.3	143.0	2.348	16.186	2.480	17.102
	1581.9	10.9	626.3	2.526	17.415		
	2188.5	15.1	852.3	2.568	17.705		
6	295.2	2.0	161.5	1.828	12.603	2.029	13.993
	1421.8	9.8	667.6	2.130	14.684		
	2045.6	14.1	960.0	2.131	14.692		
7	496.6	3.4	280.6	2.381	16.414	2.474	17.056
	1388.9	9.6	569.4	2.439	16.819		
	2519.6	17.4	968.6	2.601	17.936		
8	730.6	5.0	327.9	2.228	15.363	2.324	16.026
	1505.4	10.4	643.9	2.338	16.120		
	2274.6	15.7	945.1	2.407	16.594		
9	521.5	3.6	241.3	2.161	14.902	2.297	15.841
	1505.1	10.4	643.9	2.337	16.117		
	2166.2	14.9	905.0	2.394	16.504		
10	563.3	3.9	259.5	2.171	14.967	2.256	15.557
	1411.7	9.7	611.5	2.309	15.918		
	2154.0	14.9	940.8	2.290	15.786		
11	497.7	3.4	224.4	2.218	15.293	2.255	15.547
	1461.3	10.1	656.1	2.228	15.362		
	2313.6	16.0	997.9	2.318	15.986		
12	506.6	3.5	224.8	2.254	15.538	2.311	15.931
	1387.2	9.6	605.8	2.290	15.789		
	2140.1	14.8	896.1	2.388	16.467		
13	637.1	4.4	312.1	2.041	14.075	2.097	14.457
	1429.4	9.9	692.4	2.064	14.234		
	2205.7	15.2	1009.8	2.184	15.061		
14	751.7	5.2	330.4	2.275	15.687	2.301	15.866
	1561.8	10.8	687.5	2.272	15.663		
	2318.5	16.0	983.9	2.356	16.248		
15	371.5	2.6	185.1	2.007	13.838	2.095	14.444
	1467.9	10.1	686.4	2.139	14.745		
	2267.5	15.6	1060.0	2.139	14.719		

within this limit the gauges can be used interchangeably.

The experimental program calls for measuring stress waves at three points in the frozen soil column. Thus, three sets of voltage dividers and charge amplifiers will be used. To check to see if the systems are interchangeable, we conducted additional tests by pairing charge

dividers and charge amplifiers for three separate systems, but using the same shock gauge for each paired set.

Table 6 gives the results of this test. We noticed about a 15.3% difference between the maximum and minimum values in the calibration factor data set. However, this discrepancy cannot be attributed to the instru-

Table 5. (cont'd).

Gauge no.	Input peak stress		Gauge output (mV)	Calibration factor		Average calibration factor: F	
	(lb/in. ²)	(MN/m ²)		[(lb/in. ²)/mV]	[(KN/m ²)/mV]	[(lb/in. ²)/mV]	[(KN/m ²)/mV]
Batch B							
16	1063.1	7.3	242.5	4.384	30.227	4.214	29.055
	1779.8	12.3	431.9	4.121	28.413		
	2594.3	17.9	627.1	4.137	28.524		
17	479.9	3.3	143.4	3.347	23.075	3.478	23.983
	1680.9	11.6	491.8	3.418	23.566		
	2427.6	16.7	661.4	3.670	25.307		
18	828.4	5.7	218.0	3.800	26.201	3.914	26.990
	1710.4	11.8	440.8	3.880	26.754		
	2422.1	16.7	596.1	4.063	28.016		
19	832.2	5.7	229.8	3.621	24.970	3.607	24.867
	1931.6	13.3	542.6	3.560	24.545		
	2384.2	16.4	655.3	3.638	25.086		
20	594.4	4.1	142.4	4.174	28.781	4.383	30.221
	1568.1	10.8	361.4	4.339	29.917		
	2264.6	15.6	488.5	4.636	31.964		
21	600.0	4.1	136.6	4.392	30.286	4.745	32.716
	1474.6	10.2	315.0	4.681	32.277		
	2178.5	15.0	422.1	5.161	35.586		
23	751.2	5.2	172.5	4.355	30.026	4.523	31.188
	1274.4	8.8	286.9	4.442	30.627		
	2164.6	14.9	453.5	4.773	32.911		
24	636.1	4.4	110.4	5.762	39.727	6.034	41.603
	1380.0	9.5	227.2	6.074	41.880		
	2024.5	14.0	323.1	6.266	43.203		
25	722.3	5.0	132.6	5.447	37.559	5.818	40.114
	1390.0	9.6	243.2	5.715	39.408		
	2135.1	14.7	339.4	6.291	43.375		
27	640.0	4.4	190.8	3.354	23.128	3.463	23.897
	1431.7	9.9	411.6	3.478	23.983		
	2080.1	14.3	584.8	3.557	24.525		
28	712.3	4.9	176.5	4.036	27.826	4.184	28.851
	1571.9	10.8	374.8	4.194	28.917		
	2167.4	14.9	501.3	4.324	29.811		
29	307.4	2.1	94.2	3.263	22.500	3.329	22.951
	1437.9	9.9	444.0	3.231	22.279		
	2209.6	15.2	632.9	3.491	24.072		

Table 6. Interchangeability of interface instrumentation.

Gauge no.	Charge divider no.	Charge amplifier no.	Impact stress		Gauge output (mV)	Calibration factor	
			(lb/in. ²)	(MN/m ²)		[(lb/in. ²)/mV]	[(KN/m ²)/mV]
5	1	1	607.2	4.2	241.5	2.514	17.336
			1518.5	10.5	683.1	2.223	15.327
			2348.6	16.2	1004.2	2.339	16.126
5	2	2	638.9	4.4	278.5	2.294	15.818
			1630.2	11.2	660.5	2.468	17.018
			2435.9	16.8	927.6	2.626	18.106
5	3	3	1810.9	12.5	728.9	2.484	17.130
			2399.8	16.5	962.1	2.494	17.198

mentation system alone, as even a single gauge with the same instrumentation produced about a 12% variation in the calibration factor data among impact blows. Thus, in general, a 15% scatter in the data isn't unusual when gauges and instrumentation systems are used interchangeably.

GENERAL REMARKS AND CONCLUSIONS

PVDF piezopolymer is a highly sensitive sensor material that is very good for shock or impact measurements. The material is compliant, lightweight and tough. Thus, it is vastly different from other well known piezoelectric materials, such as quartz, Rochelle salt and other piezoceramics. For application as a shock gauge it needs to be configured properly.

The high sensitivity of this material is of great advantage. A very large signal-to-noise ratio was obtained in all our tests; the output was so large that we needed to use a charge divider to reduce the output for our oscilloscope.

The greatest advantage that we found was in its low acoustic impedance (*pc* value). Its good impedance matching in soil will allow efficient energy transfer and significantly low signal distortion. With the proper selection of the polymer for encapsulation, unique impedance-matched transducers can be fabricated using this material.

The material is less expensive than other piezoelectric materials. Fabrication of the film to develop the transducer is also relatively easy.

The low-temperature properties of our gauge have not yet been evaluated, but the room-temperature prop-

erties appear to be adequate for its application as a shock gauge. We noticed that gauge output linearity degraded when viewed over a wide range of pressures. Minor variations in repeatability have also been observed from gauge to gauge. These variations can be attributed to fabricating inconsistencies and are not the result of intrinsic variations in material properties. For very precise measurements, individual gauge calibration will be needed. For shock wave measurements in frozen soil, the gauges will need to be individually calibrated at low temperatures and in the expected range of shock wave loading.

LITERATURE CITED

Cady, W.G. (1946) *Piezoelectricity*. New York: McGraw-Hill, p. 701.
 Chatignij, J.V. and L.E. Robb (1986) Piezofilm sensors. *Sensors*, May.
 Lovinger, A.J. (1982) In *Developments in Crystalline Polymers* (D.C. Basset, Ed.). London: Applied Science Publishers.
 Kawai, H. (1969) The piezoelectricity of PVDF. *Japanese Journal of Applied Physics*, 8: 975.
 Bergman, J.G., J.H. McFee and G.R. Crane (1971) Pyroelectricity and optical second harmonic generation in PVDF films. *Applied Physics Letters*, 18: 203.
 Pennwalt Corporation (1983) Kynar piezofilm, technical manual. King of Prussia, Pennsylvania.
 Dutta, P.K., D. Farrell, and J. Kalafut (1987) The Hopkinson bar apparatus. USA Cold Regions Research and Engineering Laboratory, Special Report 87-24.

